Incipient Failure Detection of Space Shuttle Main Engine Turbopump Bearings Using Vibration Envelope Detection

Charles B. Hopson

Rotor bearing defects are difficult to detect by traditional signal analysis techniques because the small amplitude, low frequency information is often masked by noise. This is especially true when trying to detect SSME turbopump damage from externally mounted accelerometer data. However, vibrations induced by defects often excite natural frequencies of neighboring structures, in effect, amplitude modulating the defect signature onto a structural resonance carrier frequency. By using a Vibration Envelope Detector to demodulate the information from the resonance carrier, a new low frequency spectrum can be obtained that may display an impact repetition rate, characteristic of the defect.

This paper discusses the results of an analysis performed on seven successive SSME static test firings, utilizing envelope detection of external accelerometer data. The results clearly show the great potential for using envelope detection techniques in SSME Incipient Failure Detection.

INTRODUCTION

High Pressure Oxygen Turbopump (HPOTP) bearing failure is a potentially catastrophic event capable of causing the loss of the Shuttle vehicle. Incipient Failure Detection (IFD) of HPOTP bearings must meet several requirements to be successful. It must be reliable and consistent for all engines and pumps. To insure bearing health during a flight, it must provide ample warning of bearing failure to allow safe engine shut-down. The technique should also have a minimum impact on cost and existing hardware. In addition to safety concerns, IFD would allow the maximum service of a turbopump before disassembly and inspection became necessary. IFD would also be a valuable tool in the improved design of turbopump components by monitoring the progression and characteristics of bearing degradation leading to failure.

The analysis of SSME turbopump data for indicators of bearing damage is difficult for several reasons. The severe noise environment makes the search for low amplitude, low frequency signatures nearly impossible with traditional techniques. Internal strain gages have proven to be very good for identification of

337

defects, but they are prone to failure and are not available on flight engines.

External accelerometers are common to both static and flight engines, however, the transmission of information from the bearings to the outside of the case is usually weak and buried in random noise. Additionally, the low pass filtering of the data during acquisition precludes the identification of higher frequency signatures such as inner and outer race defects.

This paper describes the results of an analysis conducted on seven successive SSME static test firings, using Vibration Envelope Detection (VED) to identify the bearing cage frequency of a HPOTP.

VIBRATION ENVELOPE DETECTION

The power spectrum of an accelerometer mounted on a rotor casing will ideally display a peak that is characteristic of a particular bearing defect. For example, an outer race defect will have a characteristic signature because of the repetitive impacting of balls on the defect. The impacting frequency is dependent upon the number of balls, the outer race diameter, rotational speed, etc. The signatures are difficult to detect because they are normally low frequency and low amplitude, often obscured by random noise. However, the impacting sometimes excites modes of neighboring structures, in effect, amplitude modulating the defect signature onto a modal resonance (carrier frequency). These carriers are higher in frequency that the defect frequency and two advantages are realized. Firstly, random noise is usually lower at high frequencies and secondly, for a fixed displacement, acceleration amplitude is proportional to the square of the frequency. To illustrate, assume a harmonic displacement of the form

$$x(t) = A \sin \omega t \tag{1}$$

where A is the peak amplitude and ω is the frequency. Differentiating twice results is an acceleration of the form

$$\ddot{x}(t) = -\omega^2 A \sin \omega t \tag{2}$$

Solving both equations for A sin ωt and equating,

$$\ddot{x}(t) = -\omega^2 x(t) \tag{3}$$

Hence, for a given displacement, acceleration is proportional to the square of the frequency.

Now assume that the amplitude of the defect signature is given by

$$V_D(t) = A_D \cos \omega_D t \tag{4}$$

where A_D is the peak amplitude and ω_D is the impacting frequency due to the defect. The amplitude of the structural resonance carrier can be described by

$$V_R(t) = A_R \cos \omega_R t \tag{5}$$

where A_R is the peak amplitude of the resonance and ω_R is the carrier frequency. Excitement of the structural mode by the impacting causes the resonance carrier amplitude to vary with the instantaneous magnitude of the defect signature.

Therefore, the instantaneous carrier amplitude becomes

$$A_C(t) = A_R + A_D \cos \omega_D t \qquad (6)$$

resulting in an amplitude modulated (AM) wave given by

$$V_{AM}(t) = (A_R + A_D \cos \omega_D t) \cos \omega_R t$$

$$= A_R(1 + m \cos \omega_D t) \cos \omega_R t \qquad (7)$$

where $m \equiv A_D/A_R$ is the depth of modulation. Equation (7) can also be expressed as

$$V_{AM}(t) = A_R \cos \omega_R t + \tfrac{1}{2} m A_R(\omega_R + \omega_D)t + \tfrac{1}{2} m A_R(\omega_R - \omega_D)t \qquad (8)$$

So the AM wave spectrum contains peaks at the structural resonance carrier frequency and at the difference frequencies $\omega_R + \omega_D$ and $\omega_R - \omega_D$ (upper and lower side frequencies). Thus, the spectrum contains the defect signature information, but centered around a higher frequency determined by the resonance of the excited structural mode.

The VED technique uses a band pass filter, centered around the resonance carrier, to filter out everything except the carrier and side frequencies, then outputs the envelope of this signal (the demodulated signal), resulting in a new low frequency spectrum containing the defect signature, free of the obscuring noise.

It should be understood that the enhanced spectrum will still contain the noise not filtered out before enveloping, but it will be much less than that in the original unprocessed spectrum. Ideally, the band pass filtered signal should contain the carrier and both sidebands. This means that the filter bandwidth must be twice that of the defect frequency of interest. A smaller bandwidth will attenuate the sidebands, decreasing the effectiveness of the technique. A bandwidth larger than twice the modulating impact frequency will allow excessive noise into the envelope detector. Noise between the side frequencies and the carrier will be introduced in either case, as will noise outside of the band due to finite filter roll off.

In this analysis a B&K constant percentage bandwidth tracking filter was used in conjunction with a Shaker Research Model 223A Vibration Envelope Detector.

DATA DESCRIPTION AND OBJECTIVE

This study was conducted on SSME Static Tests 406, 407, 408, 409, and 410 on the A2 Test Stand and Tests 283 and 284 on the A3 Test Stand. These tests were chosen because HPOTP #0307 was used on all seven firings and a high 2X cage frequency became apparent on Test 410. Internal strain gages installed on the pump,

failed before Test 283; however, the data acquired previous to Test 283 were useful for verifying that the cage signatures extracted by envelope detection were, in fact, real. In other words, when the VED technique extracted cage signatures that were not seen in the original spectra, the frequencies from the internal strain gage spectra and the VED spectra matched, thereby confirming that the technique was not producing false data.

The objective of the study, though, was to investigate the feasibility of using VED on external accelerometers. Considerable time was spent on Test 410 because it was known to have a high 2X cage signature. If a procedure could be found to extract the cage signature from Test 410 using VED, then the same procedure would be used on tests prior and subsequent to Test 410. A further objective, assuming a consistent procedure could be developed, was to determine if the amplitude of the cage signature or its harmonics would be useful in tracking the bearing degradation with time.

Before the study began, it was believed that the best measurement for analysis would be accelerometer PBP RAD 135-2: a radial accelerometer on the preburner pump. Experience later proved this assumption to be correct. PBP RAD 135-2 data are recorded at 60 ips and have a cut-off frequency of 2.5 kHz. For VED analysis, the frequency range must be at least twice as high as the defect frequency of interest. This fact alone precluded the search for inner and outer race defects. In fact, the frequency range should be upwards of 40 kHz to expect the successful detection of race defects. The cage signature, however, is much lower (~205 Hz); so this became the frequency of interest. It should be noted that even though PBP RAD 135-2 is filtered at 2.5 kHz, the rolloff is shallow enough that higher frequencies can be analyzed, although this ability diminishes rapidly.

Unfortunately, after Test 410, HPOTP #0307 was installed on an engine at the A3 Test Stand. This made comparison more difficult because the engine characteristics are somewhat different and it was discovered that the data filter rolloffs are considerably different making amplitude comparisons of peaks above 2.5 kHz disagree between test stands.

While this analysis could never be expected to detect all bearing defects (due to the limitations in the data recordings), it was hoped that it would demonstrate the feasibility of the VED technique and warrant further study.

DISCUSSION OF ANALYSIS PROCEDURE

The analysis began by reviewing the analog tape recording of PBP RAD 135-2 on Test 410, since it was known to contain a high 2x cage frequency. The tape output was connected to the constant percentage bandwidth tracking filter and the output of the filter was then fed into the Vibration Envelope Detector for demodulation. This envelope was then displayed on a spectrum analyzer. The bandwidth of the tracking filter was adjusted during the analysis so that it would be at least equal to but not much greater that 420 Hz (two times the cage frequency). As stated before, this allows the AM wave to be enveloped but keeps the noise to a minimum. As the tape was shuttled back and forth, the spectrum analyzer was monitored for cage signatures as the tracking filter was swept through the frequency range of the measurement.

As the analysis progressed, strong cage and cage harmonic peaks appeared on the spectrum analyzer when the center frequency of the filter got to around 6700 Hz. This indicated that the cage signatures were being carried on a signal in this frequency range. By increasing the tracking filter bandwidth, cage multiples out to the seventh harmonic were observed. The 6700 Hz frequency range then became the focus during the remainder of the analysis. Figure 1 shows the basic flow and a comparison of an original unprocessed spectrum and a VED enhanced spectrum. Note the absence of cage signatures in the original spectrum, while the enhanced spectrum contains the cage frequency plus the second and third harmonics.
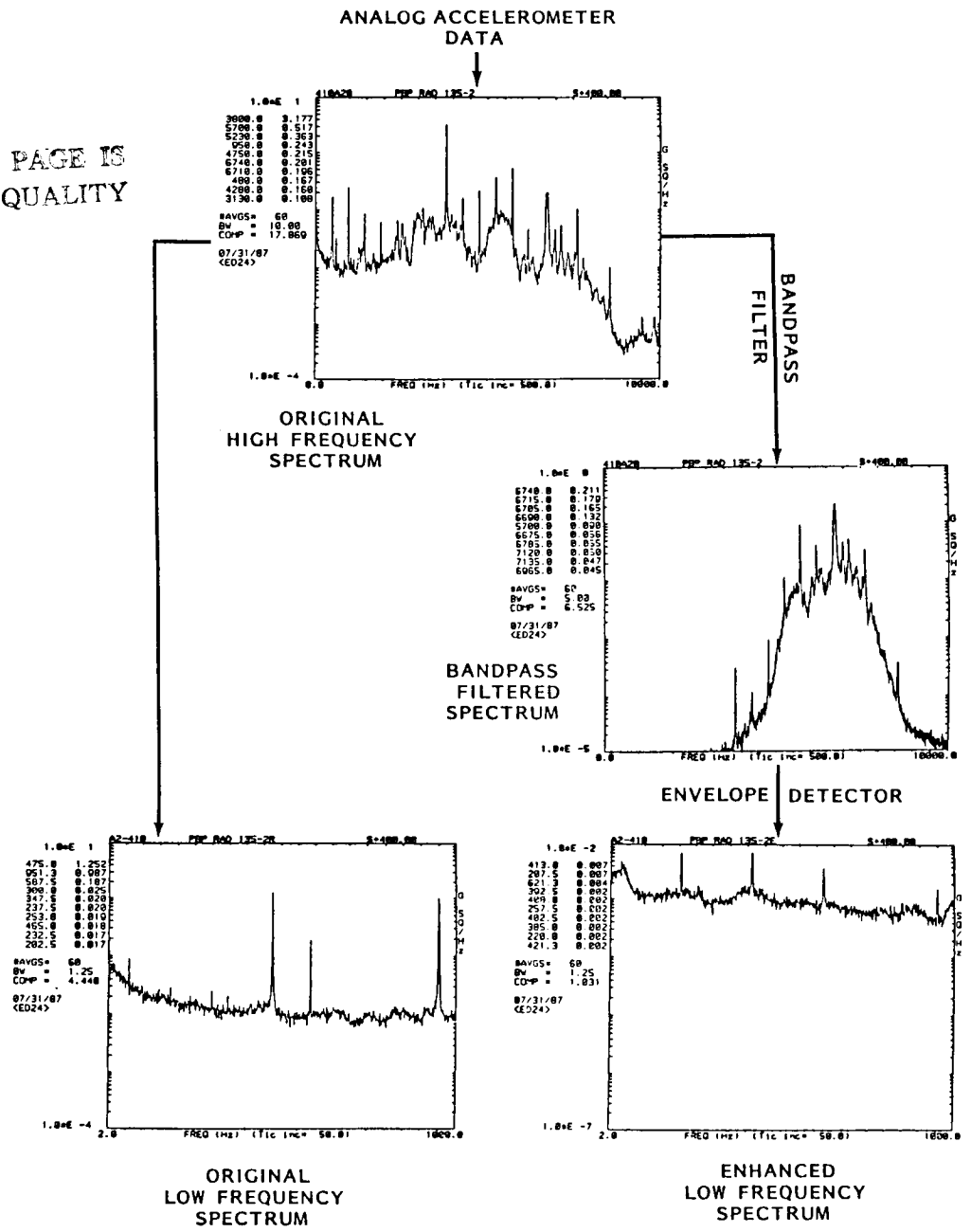
FIGURE 1   ENVELOPE DETECTION FLOW DIAGRAM

After the cage signature was extracted from the 6700 Hz carrier, a comparison was made between spectra from Tests 406 and 410. Since Test 406 was the first analyzed, it was used to baseline the characteristics of an undamaged bearing. When compared, a large anomalous peak can be seen on the spectrum of Test 410 that is absent on Test 406. This comparison is shown in Figure 2. In the PSD from Test 410, an upper side frequency corresponding to the fundamental cage is also clearly observed.

Figure 3 shows a summary of the spectra from Tests 407 through 410, analyzed using a 1500 Hz bandpass filter centered at 6750 Hz. The plots on the left are the original spectra from each test averaged over the time that the engine was running at 104% of the Rated Power Level (RPL). The plot to the right of each spectrum is the corresponding enhanced spectrum. Each pair of spectra was processed identically except that the enhanced spectra were processed after the signal was filtered, enveloped, and passed through an adaptive filter. The adaptive filter provides spectral line enhancement by adaptively building narrow bandpass digital filters around each line, reducing random noise. The adaptive filter was utilized in this study for peak identification, but was not used for amplitude analyses.

FIGURE 2   POWER SPECTRAL DENSITY COMPARISON OF TESTS 406 AND 410

The original spectra show the HPOTP synchronous frequency peak and harmonics, however peaks at the bearing cage frequency are not observed. Because of the enhancement, though, the cage signature becomes apparent. The spectra of subsequent tests show the cage signature increasing as bearing degradation advances. The cage harmonics become pronounced on Test 408 and increase in amplitude on Tests 409 and 410.

It was determined, after experimentation, that the optimum filter bandwidth for the analysis was around 1 kHz. This bandwidth allowed the cage and second harmonic to be demodulated with a minimum amount of noise introduced into the detector. This bandwidth, centered at 6750 Hz, was then used for the detailed analysis of all seven tests.

The VED analysis was conducted only during periods of constant engine power level so that amplitude and frequency comparisons could be made. Figure 4 is the time history of the HPOTP synchronous frequency over all seven tests. HPOTP speed changes are observed even at constant power level, due to LOX venting. Also, note that the synchronous frequency during Tests 283 and 284 is higher than on the previous five tests due to the different SSME on which the HPOTP was installed.
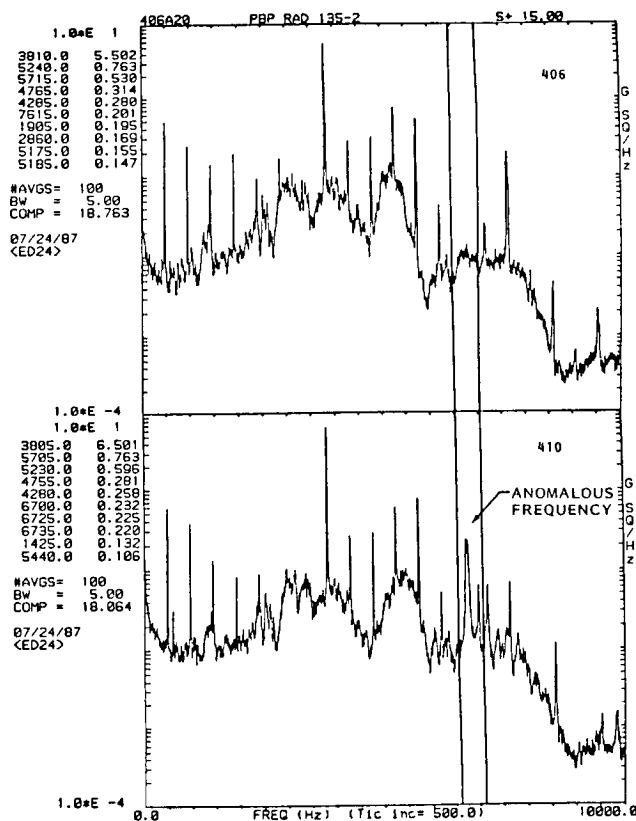
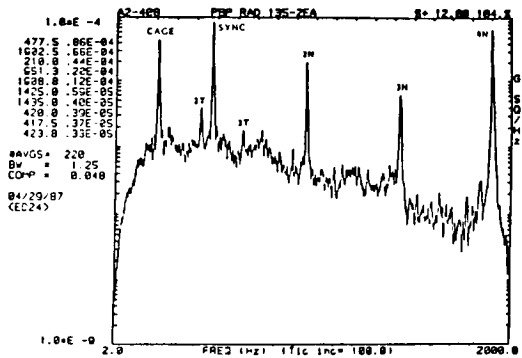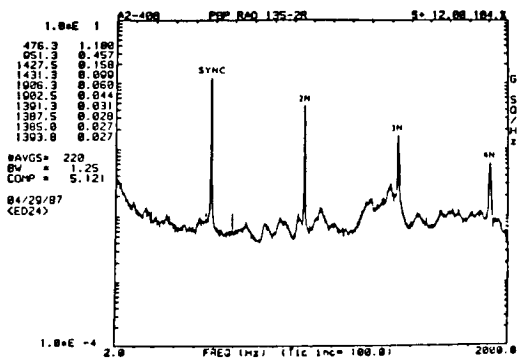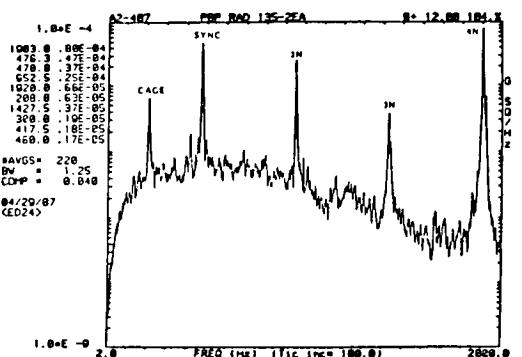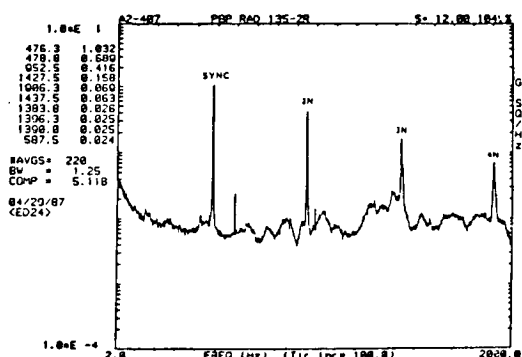ORIGINAL RAW SPECTRA   VED ENHANCED SPECTRA
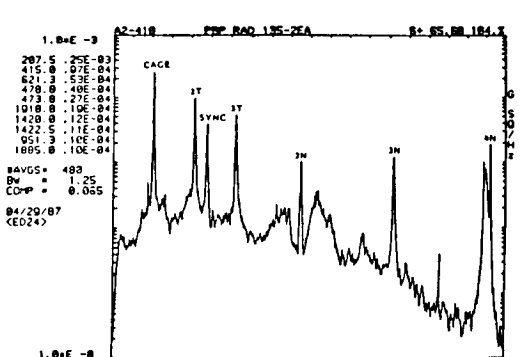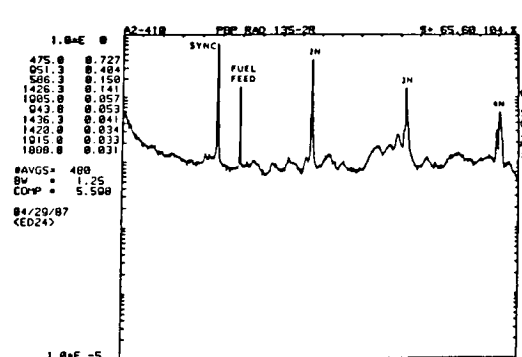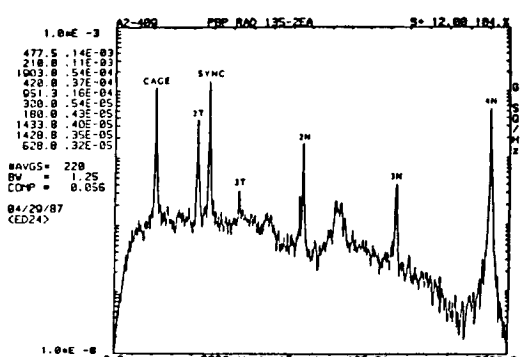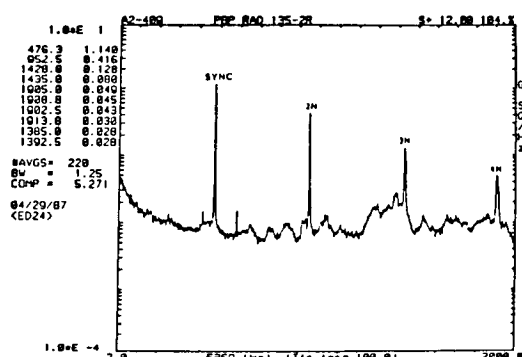
FIGURE 3   COMPARISON OF ORIGINAL SPECTRA AND
VED ENHANCED SPECTRA

Figure 5 is the time history of the anomalous carrier frequency. Observe that the frequency varies in correspondence to the synchronous frequency, indicating that it is not a resonance at all, but a response dependent on pump speed. Figure 6 is the time history of the ratio of the anomalous carrier to synchronous frequency. The ratio is shown to wander somewhat with changes in synchronous speed, however, it is in the vicinity of 14.2 times synchronous.

The anomalous carrier frequency abruptly disappeared seventy seconds into Test 283, and the ability to extract cage signatures by VED was lost. The source of the anomalous frequency has not been determined; however, it is nearly in the range where one might expect to find the second harmonic of an inner race defect signature. In fact, in the spectral analysis, there was an indication of a fundamental peak around 7.1 times synchronous which appeared to be related to the anomalous frequency; however, it was weak and sporadic. Actually, an inner race defect on a HPOTP bearing would be expected to be around 7.4 times synchronous and the disappearance of the anomalous frequency makes it even more puzzling.
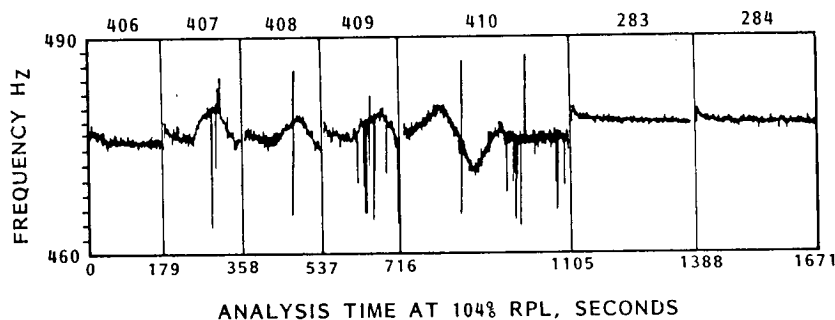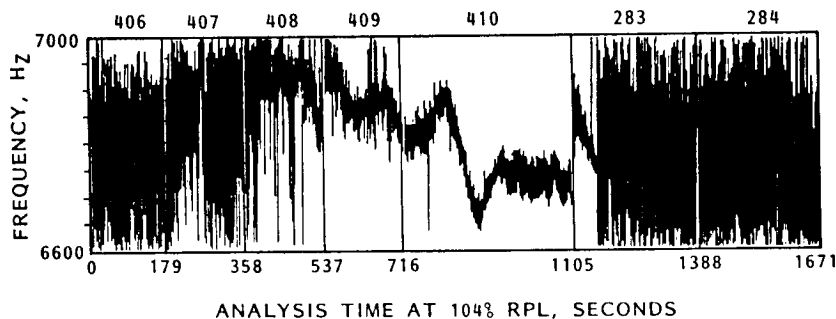
FIGURE 4   TIME HISTORY OF SYNCHRONOUS FREQUENCY

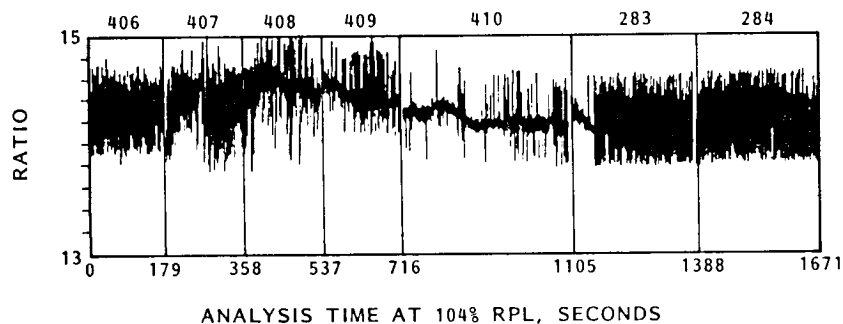FIGURE 5   TIME HISTORY OF ANOMALOUS CARRIER FREQUENCY

FIGURE 6   RATIO OF ANOMALOUS CARRIER FREQUENCY
TO SYNCHRONOUS FREQUENCY

344

Routine data processing procedures had not revealed the anomalous frequency, probably because it is in a frequency range not observed in routine data analysis. The event during Test 283 which caused the disappearance of the anomalous frequency has not been identified and without speculating on the cause, results from the VED analysis will be discussed here.

Referring back to Figure 6, note that although the ratio wanders during changes in pump speed, it is otherwise steady. The only exception is just before the anomalous event during Test 283. Here it is shown to decrease even though the pump speed was constant, possibly indicating the onset of a failure.

Figure 7 shows the time history of the anomalous frequency amplitude. Note how the amplitude increases as bearing degradation advances until the anomalous event, when the peak completely disappears.
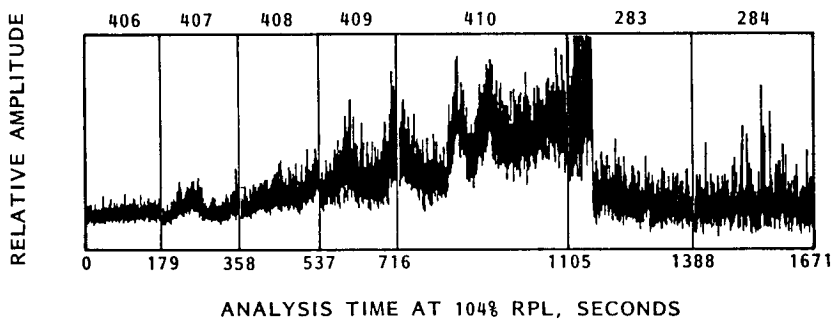

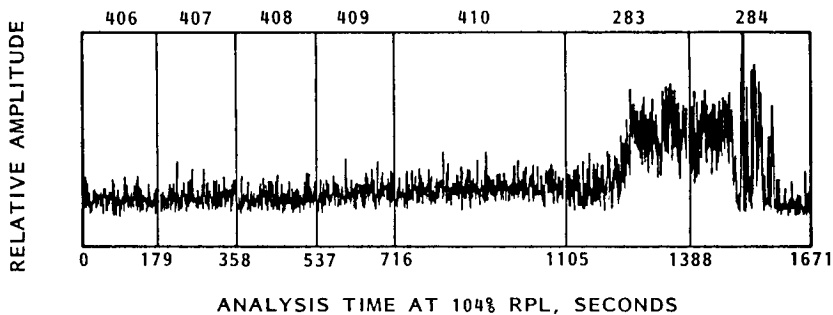FIGURE 7   RELATIVE AMPLITUDE OF ANOMALOUS FREQUENCY

FIGURE 8   RELATIVE AMPLITUDE OF 2X CAGE FREQUENCY
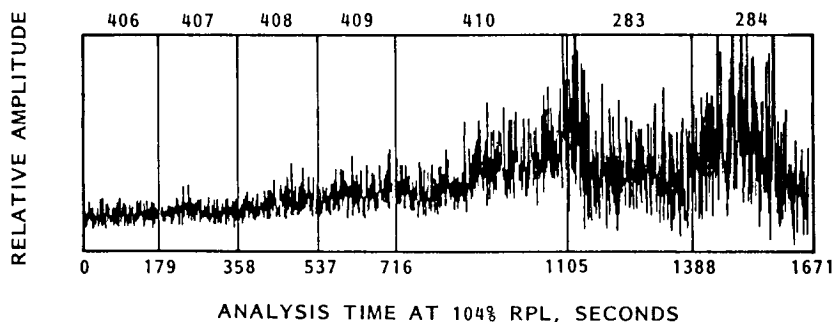(ORIGINAL SIGNAL)

FIGURE 9   RELATIVE AMPLITUDE OF 2X CAGE FREQUENCY
(ENHANCED SIGNAL)

345

Figure 8 shows the time history of the second cage harmonic amplitude. During the first five tests, the amplitude is constant because the low amplitude cage signal is buried beneath the random noise. However, after the anomalous event, the amplitude increases dramatically, possibly caused by the event. Also note that the harmonic disappeared during Test 284. The rapid disappearance, indicating a significant event had occurred, prompted the disassembly and inspection of the pump.

The inspection revealed severe ball wear and pitting. The cage was almost completely destroyed and the unconfined balls showed signs of violent impacting. The bearing also showed signs of heavy side loads and outer race spinning.

Figure 9 is the time history of the second cage harmonic amplitude processed from the VED enhanced signal. Observe the steady increase in amplitude with time. This plot is very encouraging, because while the anomalous frequency may be an effect from some other problem and probably not always indicative of bearing failure, the 2x cage signature may be an accurate measure of a cause. Note that Figures 8 and 9 were constructed using identical processing parameters, except that the signal was sent through the filter and detector before it was digitized for Figure 9. Figure 8 gives no indication of bearing failure until about 1250 seconds into the analysis, while the amplitude is seen to begin increasing hundreds of seconds earlier in Figure 9, because of the great increase in signal-to-noise ratio due to VED.

CONCLUSIONS

The results presented in this paper are encouraging and support the theory that Vibration Envelope Detection may be a feasible diagnostic method for incipient failure detection of SSME turbopump bearings. The VED method revealed evidence of HPOTP bearing degradation in a series of static test firings much earlier than did routine data analysis, utilizing data from the same existing external accelerometer. While the success in this case was dependent upon an anomalous frequency of unknown origin, the tremendous amount of additional information contained in the data was clearly demonstrated and further study is therefore justified.

RECOMMENDATIONS

This study has clearly demonstrated the ability to retrieve useful diagnostic information by using VED; however, the potential for greater success is dependent upon the frequency range of the data. VED is a procedure that works best on high frequency resonances. For example, it is possible to detect very small displacements by enveloping the impact excited resonance of an accelerometer in the 50 kHz range. The only consistent, reliable IFD technique would be the use of VED on a resonance which not only contains the defect information, but which is also assured of being uniform in frequency and character. By increasing the frequency range of the data to 80 kHz, an exhaustive investigation could be initiated possibly leading to a real-time monitoring system. Until the frequency range is increased the capabilities of VED will not be realized.

ACKNOWLEDGEMENTS

REFERENCES

1   Operation Manual, Vibration Envelope Detector Model 223A, Shaker Research Corporation, Latham, New York.

2   Swanson, W. L., "Waveform and FFT of Radially Loaded Ball Bearings with Nonuniform Ball Wear", Technical Memorandum, TM-68101-1, Wyle Laboratories, Huntsville, Alabama, April 1987.